

Seismic performances of centrifugally-formed hollow-core precast columns with multi-interlocking spirals

Jin-Ha Hwang^{1a}, Deuck Hang Lee^{2b}, Jae Yuel Oh^{1c},
Seung-Ho Choi^{1d}, Kang Su Kim^{*1} and Soo-Yeon Seo^{3e}

¹ Department of Architectural Engineering, University of Seoul,
163 Seoulsiripdae-ro, Dongdaemun-gu, Seoul 02504, Republic of Korea
² Department of Civil and Environmental Engineering, University of Illinois
at Urbana-Champaign, 205 N. Mathews Ave. Urbana, IL 61801, USA
³ Department of Architectural Engineering, Korea University of Transportation,
50 Daehak-ro, Chungju-si, Chungbuk 27469, Republic of Korea

(Received June 08, 2015, Revised January 08, 2016, Accepted February 16, 2016)

Abstract. A precast composite column system has been developed in this study by utilizing multi interlocking spiral steel into a centrifugally-formed hollow-core precast (CHPC) column. The proposed hybrid column system can have enhanced performances in the composite interaction behavior between the hollowed precast column and cast-in-place (CIP) core-filled concrete, the lap splice performance of bundled bars, and the confining effect of concrete. In the experimental program, reversed cyclic loading tests were conducted on a conventional reinforced concrete (RC) column fabricated monolithically, two CHPC columns filled with CIP concrete, and two steel-reinforced concrete (SRC) columns. It was confirmed that the interlocking spirals was very effective to enhance the structural performance of the CHPC column, and all the hollow-core precast column specimens tested in this study showed good seismic performances comparable to the monolithic control specimen.

Keywords: hollow column; precast concrete; interlocking spiral; seismic behavior; composite

1. Introduction

Compared to the conventional reinforced concrete (RC) method, the precast concrete (PC) method is significantly advantageous for construction time reduction, quality control, and minimization of constructional dust and environmental waste at construction sites (Seckin and Fu 1990, Khaloo and Parastesh 2003, Ertas *et al.* 2006, Teeuwen *et al.* 2010, Im *et al.* 2013, Ju *et al.* 2014, Lee *et al.* 2013a, b, Lee *et al.* 2014a, b). Most existing PC production facilities, however, still utilize labor-intensive production methods. In recent years, many efforts have been made to

*Corresponding author, Professor, E-mail: kangkim@uos.ac.kr

^a Ph.D. Candidate, E-mail: jinhawang@uos.ac.kr

^b Research Professor, E-mail: dlemrgod@illinois.edu

^c Ph.D. Candidate, E-mail: hahappyppy@uos.ac.kr

^d Ph.D. Candidate, E-mail: ssarmilmil@uos.ac.kr

^e Professor, E-mail: syseo@ut.ac.kr

improve such a traditional production system in the PC industry (Cuenca and Serna 2013, Hawkins and Ghosh 2006, Lárusson *et al.* 2013). In particular, as shown in Fig. 1, the centrifugally-forming method can maximize the productivity of precast concrete members by introducing an automated production process, and can provide high-quality concrete by utilizing the centrifugal forces induced in the section forming process (Seo *et al.* 2008, Lim *et al.* 2014). The centrifugally-formed hollow-core precast (CHPC) column can reduce the material usage and self-weight by the introduction of a hollow-core in the cross-section, thereby lifting load and transportation cost can also be reduced.

Fig. 2 shows the CHPC column developed in this study, and, as shown in Fig. 2(a), the ductility and strength of the proposed CHPC column system can be enhanced compared to the conventional precast column system by confining the cast-in-place (CIP) concrete filled in the hollow-core using the main interlocking spiral steel instead of the conventional hoop reinforcements (Yin *et al.* 2011, Ou *et al.* 2014). In addition, the composite performances between the CHPC column and the core-filled CIP concrete can be enhanced by employing the sub-interlocking spiral steel together with the strong confining effect on the lap-spliced reinforcements



(a) Pre-fabricated bars



(b) Assembling mold



(c) Placing concrete and rotating mold



(d) Steam curing

Fig. 1 Manufacturing process of centrifugally-formed hollow-core precast (CHPC) column

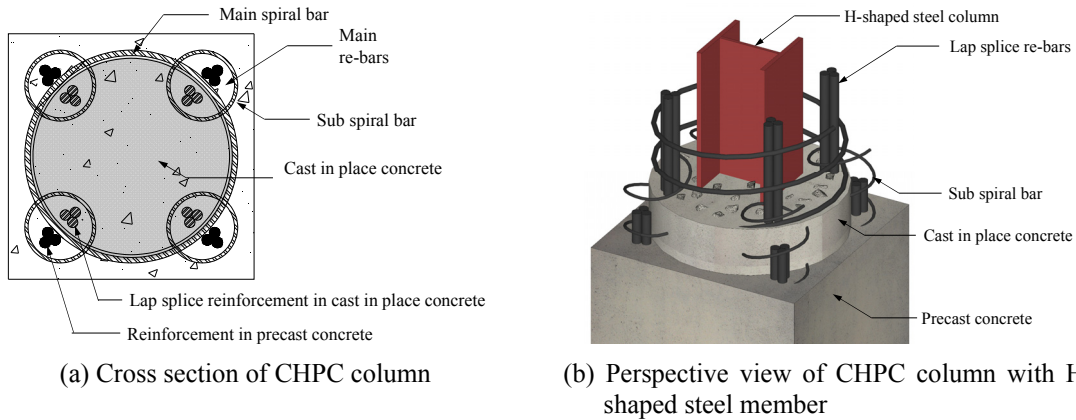


Fig. 2 Cross sectional and perspective view of CHPC columns

at precast concrete column-foundation connections. The wide flange steel column can be inserted into the hollow-core, as shown in Fig. 2(b), to build a steel-reinforced concrete (SRC) composite mega column system, which can be used in high-rise buildings.(Xue *et al.* 2009, Choi *et al.* 2012, Lu *et al.* 2014) In this study, reversed cyclic lateral loading tests were carried out for both the precast concrete composite columns and the steel-concrete composite columns with the lap splices of bundled longitudinal steel bars and multi-interlocking spiral steel, and their seismic performances were assessed and discussed in detail.

2. Test program

The details of reinforcing bars and the section dimensions of the column specimens tested in this study are illustrated in Figs. 3, 4, and 5, and Table 1. A total of five specimens were fabricated and tested in this study, including a conventional RC specimen with the monolithic column-foundation connection (RCC specimen) and four CHPC composite column specimens (PCC1, PCC2, SPCC-S, and SPCC-T specimens), in which the hollow-core was filled with the CIP concrete. Among the CHPC composite specimens, two specimens (SPCC-S and SPCC-T specimens) were fabricated as steel-reinforced concrete (SRC) composite columns by inserting the wide flange steel column into the hollow core.

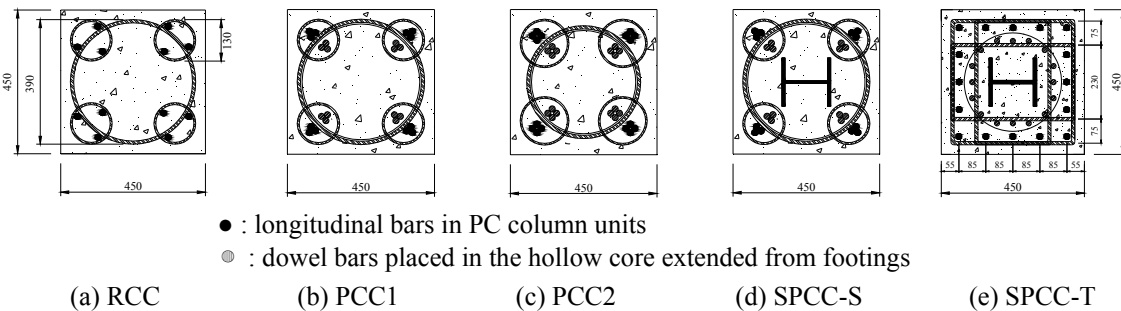


Fig. 3 Cross sections of columns with interlocking spiral bars

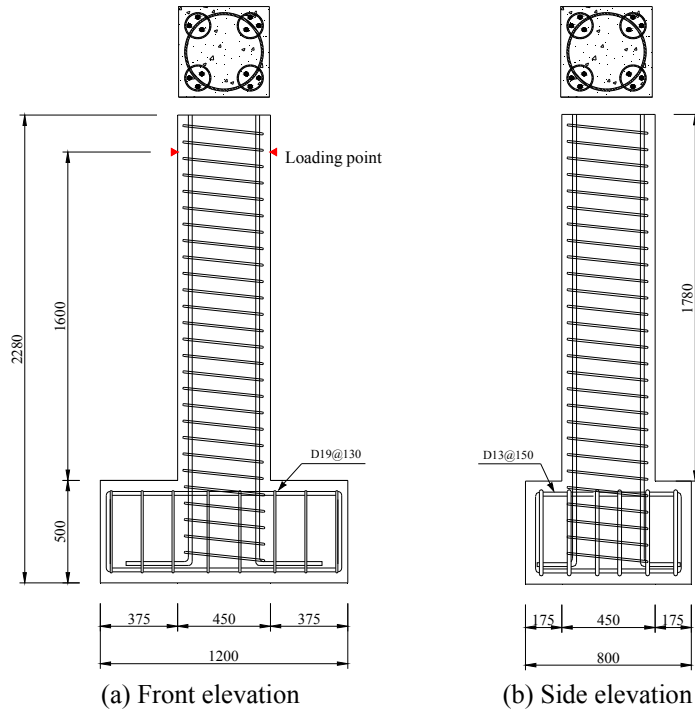


Fig. 4 Dimensions and details of RCC specimen

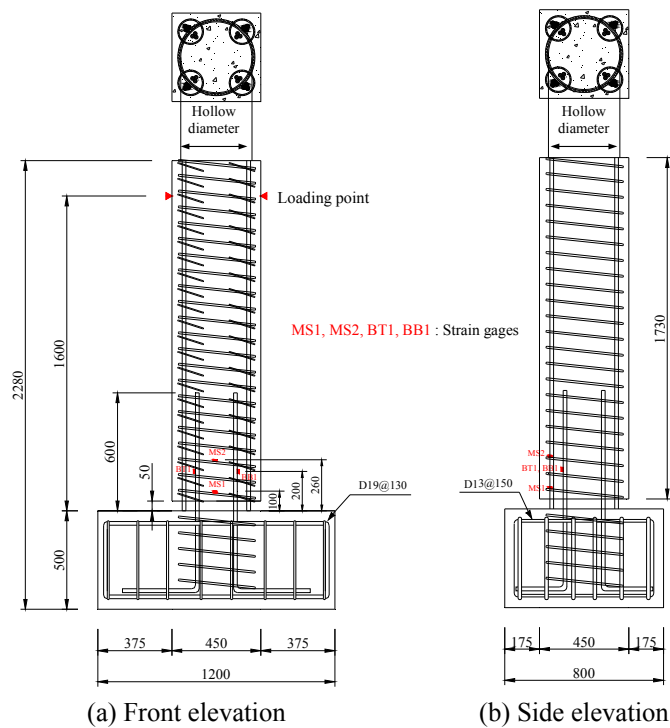


Fig. 5 Dimensions and details of PCC1 specimen

Table 1 Summary of specimens

Specimen	f'_c (MPa)		ρ_s (%)	Lap-spliced length (mm)	Confinement reinforcement		
	PC	CIP			shape	ρ_v (%)	ρ_{v2} (%)
RCC	-	42.6	1.70	-	spiral	1.62	1.08
PCC1	79.5	42.6	1.70	600	spiral	1.62	1.08
PCC2	61.7	42.6	2.26	660	spiral	1.62	1.08
SPCC-S	66.0	42.6	1.70	600	spiral	1.62	1.08
SPCC-T	76.7	42.6	1.57	450	hoop	1.58	-

ρ_s = Reinforcement ratio of longitudinal re-bars,

ρ_v = Reinforcement ratio of the main spiral bars,

ρ_{v2} = Reinforcement ratio of the sub spiral bars

For comparison, the SPCC-T specimen was transversely reinforced with the conventional hoop reinforcement details instead of the multi-interlocking spiral steel. All the specimens had square sections with dimensions of 450 mm \times 450 mm. The compressive strengths of concrete (f_c) measured at the time of testing are summarized in Table 1, and the compressive strength of CIP concrete ($f_{c,CIP}$) used for the CHPC column specimens was equal to that of the RCC specimen. As illustrated in Fig. 4, for the RCC specimen, all spiral steel reinforcements and the longitudinal reinforcements were arranged continuously from the foundation stub to the column with no splice, and the foundation stub and column parts were fabricated monolithically. All of the longitudinal reinforcements used in the RCC specimen were also placed inside of the sub-interlocking spirals, as illustrated in Fig. 3(a), and the longitudinal reinforcement ratio (ρ_l) was 1.70%.

The minimum reinforcement ratio of the spiral steel ($\rho_{s,min}$) is specified in ACI318-11 (ACI318-11 2011, Leet and Bernal 1997), as follows

$$(A_g - A_c)(0.85f'_c) \leq A_c(4.1f_3) \quad (1)$$

where A_g is the gross area of the column section, A_c is the section area of concrete confined by the main spiral steel, and f_3 is the confining stress induced by the main spiral steel. Since the additional confinements were provided on the longitudinal reinforcements and inside concrete surrounded by the sub-spirals of the proposed CHPC columns, Eq. (1) can be modified by including the concrete area confined by the sub-spirals, as follows

$$(A_g - A_c - A_{cs})(0.85f_{ck}) \leq A_c(4.1f_3) + A_{cs}(4.1f_{3s}) \quad (2)$$

where A_{cs} is the section area of concrete confined by the sub-spiral steel, f_{3s} is the confining stress induced by the sub-spiral steel, and f_3 and f_{3s} can be expressed as $2A_{sp1}f_{y1}/D_{c1}s_1$ and $2A_{sp2}f_{y2}/D_{c2}s_2$, respectively, where A_{sp1} , A_{sp2} , f_{y1} , f_{y2} , D_{c1} , D_{c2} , s_1 , and s_2 are the cross sectional area, the yield strength, the diameter, and the spacing of the main spiral and sub-spiral steel, respectively. Therefore, the minimum ratio of spiral reinforcement ($\rho_{s,min}$) required for the CHPC column specimens can be estimated by Eq. (2). In this study, the diameters of the main spiral and the sub-spirals used in all the test specimens were 13.0 mm and 6.0 mm, respectively. Accordingly, based

on Eq. (2), the pitch of the spiral bars was designed to be 80 mm, and the corresponding steel ratios of the main spiral and sub-spiral (ρ_s and $\rho_{s,sub}$) were 1.62 % and 1.08 %, respectively, as shown in Table 1.

As illustrated in Fig. 5, the CHPC column and foundation stub part of all the precast specimens were fabricated separately, and they were integrated by placing the CIP concrete into the hollow core of the PC column. The longitudinal reinforcements extended from the foundation stub to the inside of the hollow core of the PC column and those from the PC column were lap-spliced at the column-foundation connection. For the cases of the SPCC-S and SPCC-T specimens composite with the wide flange steel column, the steel columns were fastened by pretension bolts with the baseplate pre-installed on the concrete foundation. Figs. 3(b) and 3(c) show the section details of the PCC1 and PCC2 specimens. The longitudinal reinforcement ratio (ρ_l) of the PCC1 specimen was 1.70%, and this was equal to that of the RCC specimen. In addition, three bar-bundles were provided at the corner regions of the column section. The outer diameters of the main spiral and the sub-spiral steel were 390 mm and 130 mm, respectively, and the distance from the extreme fiber of the column section to the center of the bundled longitudinal reinforcements was 75.0 mm, with 30 mm of the clear concrete cover thickness. For the PCC2 specimen, the longitudinal reinforcement ratio (ρ_l) was 2.26%, and four-bar bundles were lap-spliced at the column-foundation connection as shown in Fig. 5. The diameter of the hollow-core of the CHPC column was almost equal to the inner diameter of the main spiral steel, and the area ratio of the hollow core to the concrete gross section (A_{core}/A_g) was 51.7%. The ACI318-11 code (2011) specifies that the lap splice of bundled reinforcements should be staggered to avoid all the individual bars of a bar bundle being simultaneously lap-spliced at a certain section. In addition, in chapter 21 of the ACI318-11 code, the lap splice of the reinforcement within the region of twice the effective depth of the column section (i.e., $2d_s$) from the face of the joint in the RC special moment-resisting frame was not permitted, thus the reinforcement details shown in Fig. 5 did not strictly satisfy the provisions specified in ACI318. However, a good alternative for the mechanical splicing of the bundled reinforcements has not yet been developed; the application of the staggered lap splicing to the bundled reinforcements would result in poor constructability, and it is also very difficult to use in the current precast concrete construction practice. Thus, in this study, the simple lap splicing method for bundled reinforcements without a staggered joint, in which the confinement effect of the main spiral and sub-spiral steel can be fully utilized, was introduced to the test specimens, and the performance of this lap splicing method was verified through experiments. The lap splice lengths of all the specimens were determined to satisfy the provisions specified in ACI318-11 (2011), and the PCC1 and PCC2 specimens with the three bar bundles and four bar bundles were lap-spliced at distances of 600 mm and 660 mm from the PC column-to-found connections, respectively, whose lap-spliced lengths were extended by 20% and 33% from those of single bars, respectively, according to the ACI318 provisions. Figs. 3(d) and 3(e) show the detailed section dimensions of the SPCC-S and SPCC-T specimens. Both specimens were fabricated as SRC composite columns by inserting the wide flange steel columns ($H150 \times 150 \times 10 \times 7$) into the hollow part of the CHPC columns. The details of the longitudinal and transverse reinforcements of the SPCC-S specimen were basically identical to those of the PCC1 specimen. The SPCC-T specimen was transversely reinforced by employing conventional hoop reinforcements, which was designed as an RC special moment-resisting frame specified in chapter 21 of ACI318-11, and the reinforcement ratios in the longitudinal and transverse directions (ρ_l and ρ_t) were 1.57% and 1.58%, respectively. For the SPCC-S specimen, the three-bar bundled reinforcements were lap-spliced at a distance of 600 mm from the column-foundation connection. For the case of the

SPCC-T specimen, the longitudinal bars were lap-spliced at a distance of 450 mm from the column-foundation connection, whose dowel bars were placed inside of the hollow-core of the CHPC column.

As shown in Fig. 6, a 1000 kN capacity actuator fixed on the vertical strong wall was used to apply the cyclic lateral loads, and 10% of the axial capacities of the specimens (i.e., $0.1P_n$) was introduced by using a 1400 kN hydraulic jack and 47.0 mm prestressing thread bars. The axial force was controlled constantly during testing by monitoring the strain behavior of the thread bars installed on both sides of the test specimen. It is noted that, while the lateral load was applied to the RCC specimen up to 4.0% drift ratio in the positive direction, it was applied up to 2.5% drift ratio only in the negative direction due to the unexpected damage of the loading frame apparatus during testing in the negative direction.

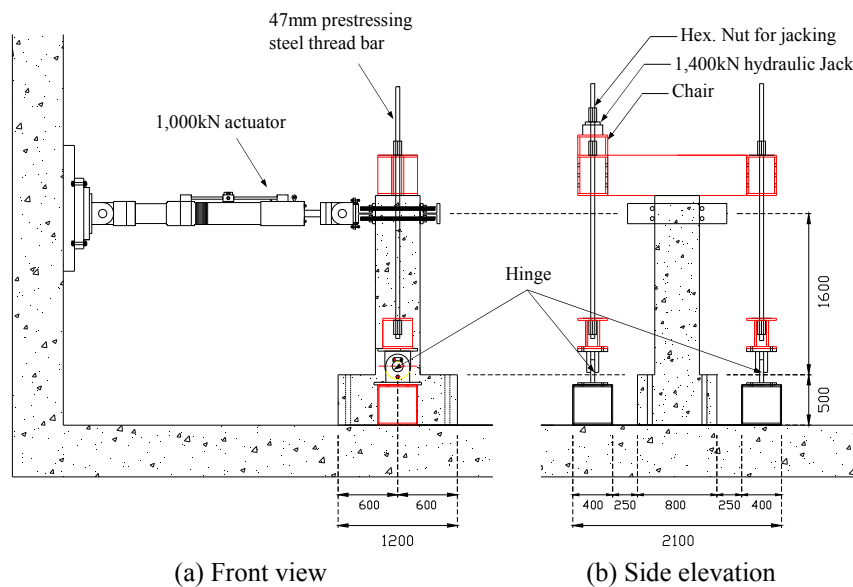


Fig. 6 Test setup

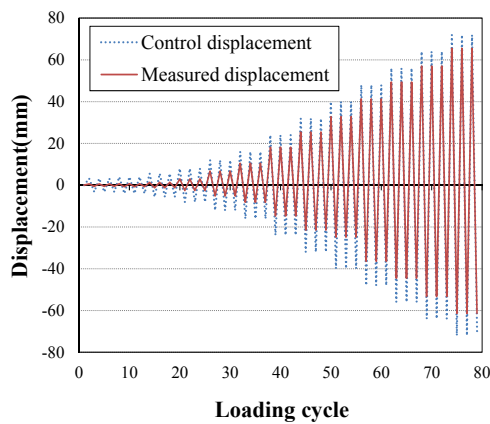


Fig. 7 Targeted and measured displacement of PCC specimen

3. Test results

As summarized in Table 2, the acceptance criteria for the RC special moment-resisting frame were proposed by the ACI committee 374 (2005), where the minimum required level of the major seismic performance indicators, such as the strength degradation, the energy dissipation, and the stiffness reduction characteristics, were presented. The relative energy dissipation ratio is defined in the ACI committee 374 (2005) as the ratio of actual to ideal energy dissipated by test module during reversed cyclic response between given drift ratio limits, which can be calculated as the ratio of the area of the hysteresis loop for the cycle considered to the area of the circumscribing parallelograms defined by the initial stiffness during the first cycle and the peak resistance during the cycle. It should be noted that the ACI acceptance criteria were actually proposed for performance evaluation of beam-column connections. There are, however, no reference that is appropriate for the evaluation of the seismic performance of the column specimens without any beam. Thus, in this study, the seismic performance of the column specimens was checked against ACI acceptance criteria in an alternative manner. The results of the cyclic loading tests conducted in this study are shown in Fig. 8, and the stiffness degradation, the deformational capacity, and the energy dissipation capacity of the test specimens are compared with the aforementioned criteria in Table 3. The RCC specimen shown in Fig. 8(a) reached the nominal flexural strength estimated by ACI code ($M_{n,ACI}$) at a drift ratio of 0.96%. The calculated nominal flexural strength ($M_{n,ACI}$) of the RCC specimen was 441.6 kN·m and the maximum lateral load ($P_{max,+}$) observed from the test was 323.4 kN, corresponding to $M_{max} = 517.4$ kN·m. At a drift ratio of 3.5%, the lateral load decreased by about 83.0% of the maximum load, which is considered as a good deformation capacity with a low strength degradation. In addition, the relative energy dissipation ratio of the RCC specimen was about 24.0%.

Table 2 Acceptance criteria represented in ACI 374 report (2005)

Section number	Specifications
9.1.1	The test module shall have attained a lateral resistance equal to or greater than E_n before its drift ratio exceeds the value consistent with the allowable story drift limitation of the International Building Code.
9.1.2	The maximum lateral resistance E_{max} recorded in the test shall have not exceeded λE_n , where λ is the specified overstrength factor for the test column.
9.1.3	For cycling at the given drift level at which acceptance is sought, but not less than a drift ratio of 0.035, the characteristics of the third complete cycle shall have satisfied the following: (1) Peak force for a given loading direction shall have been not less than $0.75E_{max}$ for the same loading direction; (2) The relative energy dissipation ratio shall have been not less than 1/8; and (3) The secant stiffness from a drift ratio of -0.0035 to a drift ratio of $+0.0035$ shall have been not less than 0.05 times the stiffness for the initial drift ratio.

E_{max} = maximum lateral resistance of test module determined from test results,

E_n = nominal lateral resistance of test module,

λ = column overstrength factor used for test module

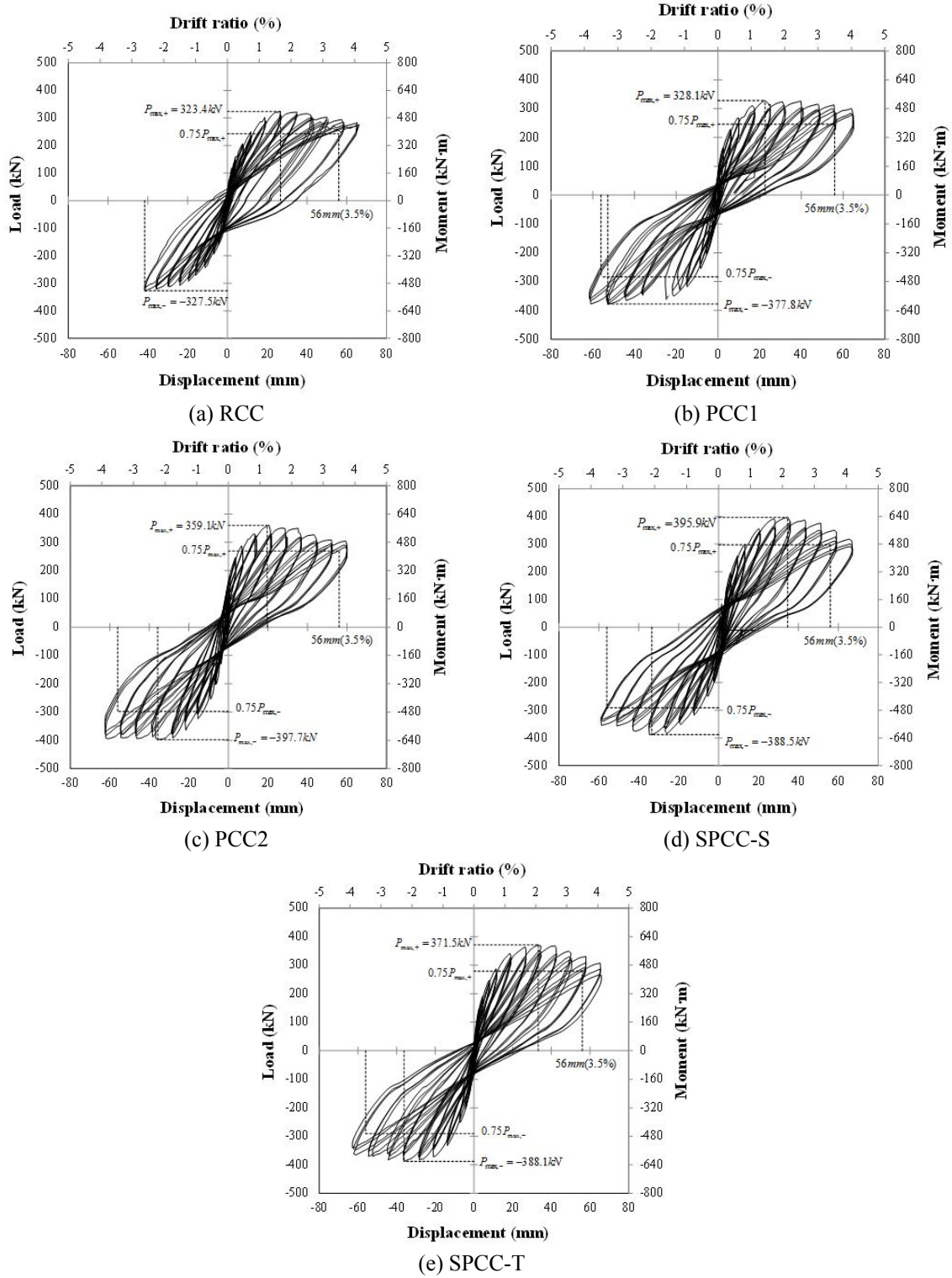


Fig. 8 Load-deflection curves

Table 3 Acceptance criteria for test specimens according to ACI 374 report (2005)

Specimen		$M_{n,ACI}$ (kN·m)	Drift ratio at M_n^* (%)	$P_{3.5\%}/P_{max}$	Relative energy dissipation ratio	K_0	K_0/K_i
RCC (CIP)	(+)	441.6	0.96	0.83	0.24	4,946	0.056
	(-)		1.10				
PCC1	(+)	456.1	0.84	0.89	0.18	4,034	0.041
	(-)		0.74	0.98			
PCC2	(+)	473.5	0.55	0.79	0.18	5,997	0.053
	(-)		0.79	0.93			
SPCC-S	(+)	541.4	1.10	0.79	0.21	6,377	0.061
	(-)		1.10	0.86			
SPCC-T	(+)	511.5	0.97	0.79	0.18	4,426	0.047
	(-)		0.80	0.91			

*IBC : allowable drift ratio = min. 1.5%

where M_n = nominal moment strength of the column

$P_{3.5\%}$ = lateral resistance of test module at the drift ratio of 3.5%

P_{max} = maximum lateral resistance of test module determined from test results

K_i = initial stiffness

K_0 = the secant stiffness from a drift ratio of -0.0035 to a drift ratio of $+0.0035$

The cyclic response of the PCC1 specimen, as shown in Fig. 8(b), shows the similar response pattern to those observed from the RCC specimen. The PCC1 specimen reached the maximum load at about a story drift ratio of 1.5% in the positive loading direction, and the load remained in a stable manner for over a 3.5% drift ratio. On the other hand, the maximum load in the negative loading direction reached at a drift ratio of 3.5%, and the lateral strength slightly increased compared with that observed in the positive loading direction. Although all the bundled reinforcements provided in the PCC1 specimen were lap-spliced at the column-foundation connection region, its seismic performance appeared to be equivalent to that of the RCC specimen without the lap splice, and pinching was barely observed in the hysteresis curve. As shown in Table 2, the PCC1 specimen satisfied all the acceptance criteria presented in the ACI374 report, except the stiffness ratio (K_0/K_i) criterion that was slightly insufficient due to its high initial stiffness (K_i). As shown in Fig. 8(b), pinching or slip behavior was not observed in the PCC1 specimen, and it can therefore be inferred that the PCC1 specimen had an acceptable seismic performance as the special moment-resisting frame.

Fig. 8(c) shows the cyclic lateral response of the PCC2 specimen, which had lap-splices of four-bar bundled reinforcements. The maximum loads (P_{max}) of the PCC2 specimen in both positive and negative loading directions was 359.1 kN and 397.7 kN, respectively, which are 10% and 5% greater than those of the PCC1 specimen in the positive and negative loading directions, respectively. This is because the longitudinal reinforcement ratio (ρ_l) of the PCC2 specimen was higher than those of the RCC and PCC1 specimens. The PCC2 specimen satisfied all the acceptance criteria presented in the ACI374 report. As illustrated in Table 3, it appeared that the ratio of load at a 3.5% drift level to maximum load ($P_{3.5\%}/P_{max}$) of the PCC2 specimen was lower than that of the PCC1 specimen. It can thus be inferred that the PCC2 specimen with the four-bar bundled reinforcements experienced greater bond loss than the PCC1 specimen reinforced by the

three-bar bundles. Nonetheless, due to the confining force provided by the multi-interlocking spirals, any sign of large bond slip or bond failure was not observed during the test.

As shown in Figs. 8(d) and 8(e), the SPCC-S and SPCC-T specimens had maximum loads at 395.9 kN and 371.5 kN in the positive loading direction and 388.5 kN and 388.1 kN in the negative loading direction, respectively, which were 20% and 15% larger than those of the RCC specimen. The SPCC-S specimen satisfied all the ACI acceptance criteria, but the SPCC-T specimen had slightly insufficient stiffness ratio (K_0/K_i) according to the ACI374 acceptance criterion, as was in the PCC1 specimen. As shown in Table 3, the relative energy dissipation of the SPCC-S specimen was about 0.21, which was equivalent to that of the RCC specimen with monolithic column-foundation connection. Such comparable performances of the SPCC-S specimen would result from the energy dissipation capacity of the steel column, the increased bond performance of the longitudinal reinforcements, and the confinement effect of the concrete provided by the interlocking spirals. In the SPCC-T specimen, as shown in Fig. 3(e), the longitudinal bars were spliced with certain distances at the column-foundation connection. The lap splice length of the longitudinal bars in the SPCC-T specimen was the shortest compared to other test specimens, because they were single bars while the others were bundled bars. The relative energy dissipation of the SPCC-T specimen was about 0.18, which was a little than that of the SPCC-S specimen with the interlocking spirals. It is, however, considered that the confined effect was developed sufficiently in the SPCC-T specimen with the conventional closed hoops, in which the H-shape steel contributed to its improved seismic performances with respect to strength, stiffness and energy dissipation.

The failure patterns of the test specimens are illustrated in Fig. 9. The RCC specimen with the monolithic column-foundation connection experienced the spalling of concrete cover in the regions located at a distance of less than 150 mm from the face of the column-foundation connection, while the damages observed in the CHPC specimens were mostly concentrated in the narrow CIP concrete between the PC column and foundation stub. In the PCC2 specimen, no severe damage was observed in the PC column except for the CIP concrete at the column-foundation connection, but the corner concrete was delaminated by up to 900 mm high from the column-foundation connection during the push-over loading after a drift ratio of 4.0 %.

According to Park and Paulay (1975), the member displacement at an ultimate lateral load, which is after the column yielded, can be calculated by integrating the curvature diagram shown in Fig. 10(c), as follows

$$\delta_u = \frac{\varphi_y l^2}{3} + (\varphi_u - \varphi_y) l_p (l - 0.5l_p) \quad (3)$$

where δ_u is the lateral displacement at the ultimate load, φ_y is the yield curvature, l is the length of the column, φ_u is the maximum curvature at the ultimate load, and l_p is the length of the plastic hinge. Since the lateral displacement at yielding of the member (δ_y) can be estimated as $\varphi_y l^2/3$, the member ductility ($\mu = \delta_u/\delta_y$) can be defined as follows

$$\mu = \frac{\delta_u}{\delta_y} = 1 + \left(\frac{\varphi_u - \varphi_y}{\varphi_y} \right) \frac{l_p (l - 0.5l_p)}{l^2/3} \quad (4)$$

Thus, the member ductility (μ) is proportional to the ductility of sectional curvature (φ_u / φ_y), and it is also proportional to the length of the plastic hinge (l_p). If the length of the plastic hinge (l_p)

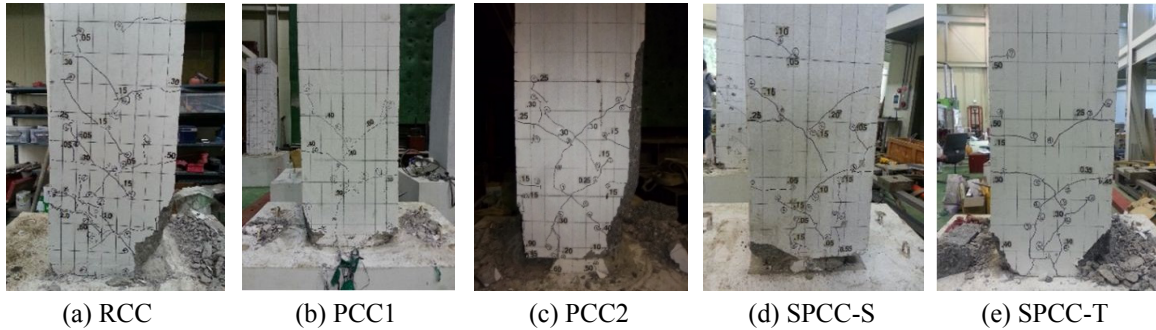


Fig. 9 Failure patterns of specimens

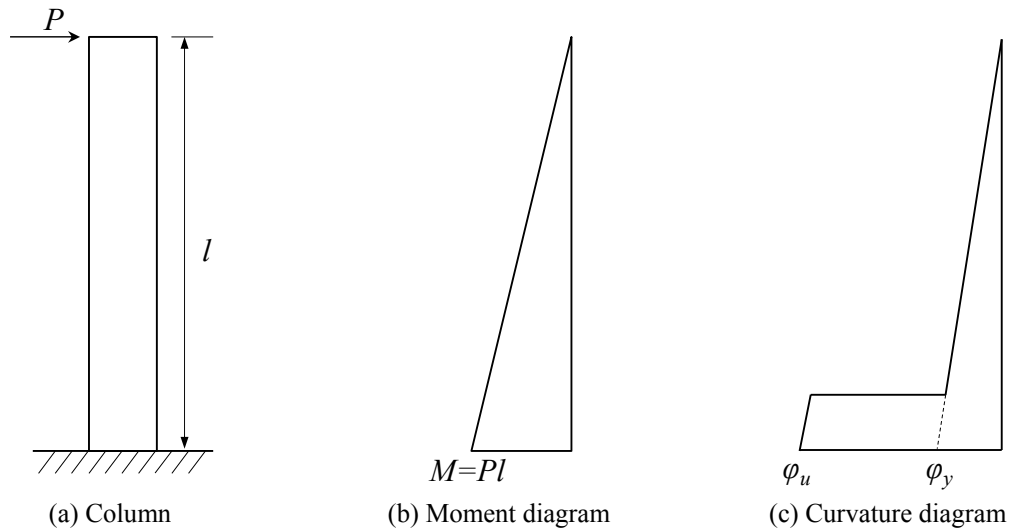


Fig. 10 Moment and curvature diagrams of column under lateral loading

is small, then the ductility of section (ϕ_u / ϕ_y) should be large enough to secure the sufficient member ductility (μ). This implies that the PC connection system is disadvantageous to achieve high ductility, because the plastic hinge lengths are expected to be small due to the concentrated deformation developed at the discrete joint regions, such as column-to-foundation or beam-to-column connections. In the CHPC composite column system proposed in this study, however, although the deformations were also concentrated at the column-foundation joint region, the sufficient ductility of sectional curvature could have been achieved, which is considered to be resulted from the multi-interlocking spirals that provided an excellent confinement of concrete and also prevented the buckling of the main reinforcements.

The strain responses measured from the longitudinal reinforcements of the CHPC composite specimens are shown in Fig. 11. The strain gauges were installed at a distance of 200 mm from the column-foundation connection, as shown in Fig. 5. The longitudinal reinforcements in all the specimens yielded or showed strains close to the yield strain, while the strains in the compression zone were relatively small. Fig. 12 shows the strain responses measured at the main spirals of the RCC and PCC1 specimens. It is noted that the strain gauges were also installed on the main spiral bar in the other specimens (i.e., PCC2, SPCC-S and SPCC-T), but unfortunately, they were

damaged during fabrication of the precast columns. The strains of the spiral bars increased in both positive and negative loading directions as the applied load increased, which means that the confining force provided by the spiral steels increased. The strains measured at the MS2 gauge mounted on the spiral bar at a distance of 300 mm from the column-foundation connection were larger than those measured from the MS1 gauge mounted at 100 mm away from the connection, which were observed in all the specimens with the spiral bars. This is because the confining force provided by the spiral steels was reduced by the concrete damage that was more severe at the closer region from the column-foundation connection. On the other hand, the maximum strain measured at the main spirals of the PCC1 specimen was about 0.0013, which was a confining stress of about 1.5 times higher than that of the RCC specimen that had the maximum strain of about 0.0008. It is considered that the lap-spliced bundled reinforcements induced larger confinement force together with the multi-interlocking spirals, from which it can be inferred that the multi-interlocking spirals had played an effective role in the CHPC composite member. In this study, 10% of the axial compressive strength of the column composite section was introduced on the specimens, and it was expected that the multi-interlocking spirals can provide a greater confinement effect when a higher axial force is applied.

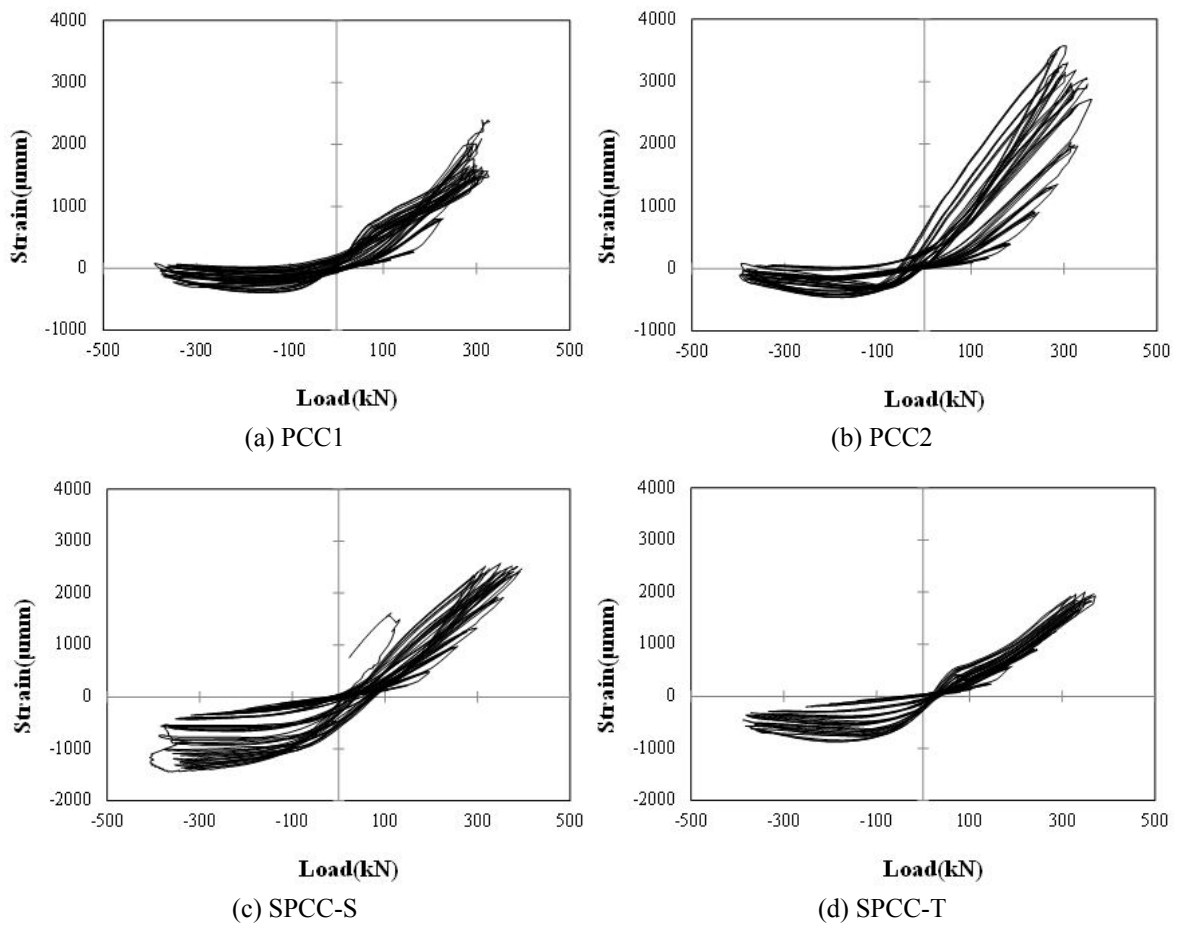


Fig. 11 Strains in longitudinal reinforcements of CHPC composite specimens

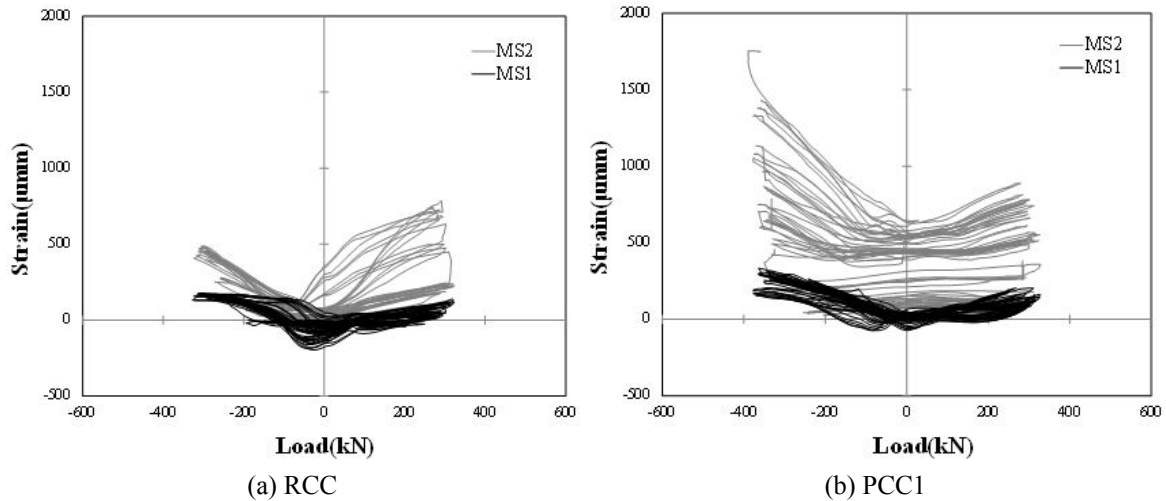


Fig. 12 Strains in main spiral bars

4. Conclusions

In this study, the CHPC composite column system utilizing the multi-interlocking spirals was proposed, and cyclic loading tests were carried out to verify its seismic performance. The test results were compared with the minimum performance requirement criteria presented in the ACI374 report. On this basis, the following conclusions were obtained.

- (1) The CHPC composite column specimens with the lap spliced bars showed the seismic performance equivalent to that of the monolithic RCC specimen with no lap spliced bars, and it was confirmed that they are applicable to building construction as a seismic force-resisting system.
- (2) All column specimens tested in this study showed excellent seismic performances, which satisfied most of the ACI acceptance criteria. Some specimens showed insufficient performances for the residual stiffness ratio criterion due to their high initial stiffness, however, no significant pinching or slip behaviors were observed during the test. It was, therefore, considered that the proposed precast composite column system can provide acceptable seismic performance as a special moment resisting frame.
- (3) The specimens lap-spliced at the PC column-foundation connections showed equivalent seismic performances compared to those without the lap splice. In addition, the CHPC composite column with the four-bar bundled reinforcements lap-spliced at the same section locations, which is not permitted in the current design provisions, also showed excellent seismic performances. It can be inferred that these comparable performances resulted from the enhanced bond performance provided by the confinement effect of the multi-interlocking spirals.
- (4) The strains of the spirals measured from the PCC specimens were apparently higher than those measured from the RCC specimen, which shows that the interlocking spirals can be utilized very effectively in the CHPC specimens with the lap splice.

Acknowledgments

This work was supported under the framework of international cooperation program managed by National Research Foundation of Korea (No. 2014K2A2A2000659).

References

- ACI Committee 318 (2011), Building Code Requirements for Structural Concrete and Commentary (ACI 318M-11), American Concrete Institute, Farmington Hills, MI, USA.
- ACI Committee 374 (2005), Acceptance Criteria for Moment Frames Based on Structural Testing and Commentary, American Concrete Institute.
- Choi, E.G., Kim, H.S. and Shin, Y.S. (2012), "Performance of fire damaged steel reinforced high strength concrete (SRHSC) columns", *Steel Compos. Struct., Int. J.*, **13**(6), 521-537.
- Cuenca, E. and Serna, P. (2013), "Failure modes and shear design of prestressed hollow core slabs made of fiber-reinforced concrete", *Compos.: Part B*, **45**(1), 952-964.
- Ertas, O., Ozden, S. and Ozturan, T. (2006), "Ductile connections in precast concrete moment resisting frames", *PCI Journal*, **51**(3), 2-12.
- Hawkins, N.M. and Ghosh, S.K. (2006), "Shear strength of hollow-core slabs", *PCI Journal*, **51**(1), 110-115.
- International Code Council (ICC) (2011), 2012 International Building Code, Country Club Hills, IL, USA.
- Im, H., Park, H. and Eom, T. (2013), "Cyclic loading test for reinforced-concrete-emulated beam-column connection of precast concrete moment frame", *ACI Structural Journal*, **110**(1), 115-126.
- Ju, H., Lee, D.H., Cho, H.C., Kim, K.S., Yoon, S. and Seo, S.Y. (2014), "Application of hydrophilic silanol-based chemical grout for strengthening of damaged reinforced concrete flexural members", *Materials*, **7**(6), 4823-4844.
- Khaloo, A.R. and Parastesh, H. (2003), "Cyclic loading of ductile precast concrete beam-column connection", *ACI Structural Journal*, **100**(3), 291-296.
- Teeuwen, P.A., Kleinman, C.S., Snijder, H.H. and Hofmeyer, H. (2010), "Experimental and numerical investigations into the composite behaviour of steel frames and precast concrete infill panels with window openings", *Steel Compos. Struct., Int. J.*, **10**(1), 1-21.
- Lárusson, L.H., Fischer, G. and Jönsson, J. (2013), "Prefabricated floor panels composed of fiber reinforced concrete and a steel substructure", *Eng. Struct.*, **46**(1), 104-115.
- Leet, K. and Bernal, D. (1997), *Reinforced Concrete Design*, (Third Edition), McGraw-Hill Co.
- Lee, J.Y., Lee, D.H., Hwang, J.H., Park, M.K., Kim, K.S. and Kim, H.Y. (2013a), "Investigation on allowable compressive stresses in pretensioned concrete members at transfer", *KSCE J. Civil Eng.*, **17**(5), 1083-1098.
- Lee, S.J., Lee, D.H., Kim, K.S., Oh, J.Y., Park, M.K. and Yang, I.S. (2013b), "Seismic performances of rc columns reinforced with screw ribbed reinforcements connected by mechanical splice", *Comput. Concrete*, **12**(2), 131-149.
- Lee, D.H., Hwang, J.H., Kim, K.S., Kim, J.S., Chung, W.S. and Oh, H.S. (2014a), "Simplified strength design method for allowable compressive stresses in pretensioned concrete members at transfer", *KSCE J. Civil Eng.*, **18**(7), 2209-2217.
- Lee, D.H., Park, M.K., Oh, J.Y., Kim, K.S., Im, J.H. and Seo, S.Y. (2014b), "Web-shear capacity of prestressed hollow-core slab unit with consideration on the minimum shear reinforcement requirement", *Comput. Concrete*, **14**(3), 211-231.
- Lim, W., Park, H., Oh, J. and Kim, C. (2014), "Seismic resistance of cast-in-place concrete-filled hollow pc columns", *J. Korea Concrete Inst.*, **26**(1), 35-46.
- Lu, X., Yin, X. and Jiang, H. (2014), "Experimental study on hysteretic properties of src columns with high steel ratio", *Steel Compos. Struct., Int. J.*, **17**(3), 287-303.
- Ou, Y.C., Ngo, S.H., Yin, S.Y., Wang, J.C. and Wang, P.H. (2014), "Shear behavior of oblong bridge

- columns with innovative seven-spiral transverse reinforcement”, *ACI Struct. J.*, **111**(6), 1339-1350.
- Park, R. and Paulay, T. (1975), *Reinforced Concrete Structures*, John Wiley & Sons, Inc.
- Seckin, M. and Fu, H.C. (1990), “Beam-column connections in precast reinforced concrete construction”, *ACI Struct. J.*, **87**(3), 252-261.
- Seo, S., Yoon, S. and Lee, W. (2008), “Evaluation of structural performance the hollow pc column joint subjected to cyclic lateral load”, *J. Korea Concrete Inst.*, **20**(3), 335-343.
- Xue, W., Yang, F. and Li, L. (2009), “Experiment research on seismic performance of prestressed steel reinforced high performance concrete beams”, *Steel Compos. Struct., Int. J.*, **9**(2), 159-172.
- Yin, S.Y., Wu, T., Liu, T.C., Sheikh, S.A. and Wang, R. (2011), “Interlocking spiral confinement for rectangular columns”, *Concrete Int.*, **33**(12), 38-45.

CC